

RESEARCH ARTICLE

# Spatial Disassociation of Disrupted Functional Connectivity for the Default Mode Network in Patients with End-Stage Renal Disease

Xiaofen Ma<sup>1</sup>✉, Junzhang Tian<sup>1</sup>✉, Zhanhong Wu<sup>2</sup>, Xiaopeng Zong<sup>2</sup>, Jianwei Dong<sup>3</sup>, Wenfeng Zhan<sup>1</sup>, Yikai Xu<sup>4</sup>, Zibo Li<sup>2\*</sup>, Guihua Jiang<sup>1\*</sup>

**1** Department of Medical Imaging, Guangdong Provincial No.2 People's Hospital, Guangzhou City, Guangdong province, PR China, **2** Biomedical Research Imaging Center and Department of Radiology, University of North Carolina at Chapel Hill, Chapel Hill, North Carolina, United States of America, **3** Department of Mathematics, Guangdong Pharmaceutical University, Guangzhou City, Guangdong province, PR China, **4** Department of Medical Imaging Center, Nanfang Hospital, Southern Medical University, Guangzhou City, Guangdong province, PR China

✉ These authors contributed equally to this work.

\* [jiangguihua177@163.com](mailto:jiangguihua177@163.com) (GJ); [zibo\\_li@med.unc.edu](mailto:zibo_li@med.unc.edu) (ZL)



CrossMark  
click for updates

## OPEN ACCESS

**Citation:** Ma X, Tian J, Wu Z, Zong X, Dong J, Zhan W, et al. (2016) Spatial Disassociation of Disrupted Functional Connectivity for the Default Mode Network in Patients with End-Stage Renal Disease. PLoS ONE 11(8): e0161392. doi:10.1371/journal.pone.0161392

**Editor:** Satoru Hayasaka, University of Texas at Austin, UNITED STATES

**Received:** February 14, 2016

**Accepted:** August 4, 2016

**Published:** August 25, 2016

**Copyright:** © 2016 Ma et al. This is an open access article distributed under the terms of the [Creative Commons Attribution License](https://creativecommons.org/licenses/by/4.0/), which permits unrestricted use, distribution, and reproduction in any medium, provided the original author and source are credited.

**Data Availability Statement:** Data are subject to ethical restrictions from the consent form for the study. The corresponding author may be contacted to request the anonymized dataset.

**Funding:** This work was supported by grants from National Natural Science Foundation of China (No. 81471639); The Science and Technology Planning Project of Guangdong Province, China (No. 2015A030313723).

**Competing Interests:** The authors have declared that no competing interests exist.

## Abstract

### Purpose

To investigate the aberrant functional connectivity of the default mode network (DMN) in patients with end-stage renal disease (ESRD) and their clinical relevance.

### Materials and Methods

Resting-state functional MRI data were collected from 31 patients with ESRD (24 men, 24–61 years) and 31 age- and gender-matched healthy controls (HCs, 21 men, 26–61 years). A whole-brain seed-based functional connectivity analysis of these collected R-fMRI data was performed by locating the seeds in the posterior cingulate cortex (PCC) and ventromedial prefrontal cortex (vmPFC) to investigate the functional connectivity of the posterior and anterior DMN over the whole brain, respectively.

### Results

Compared to the HCs, the patients exhibited significantly decreased functional connectivity with the PCC in the left middle temporal gyrus, the right anterior cingulate gyrus, and the bilateral medial superior frontal gyrus. For the vmPFC seed, only the right thalamus showed significantly decreased functional connectivity in the patients with ESRD compared to HCs. Interestingly, functional connectivity between the PCC and right medial superior frontal gyrus exhibited a significantly positive correlation with the hemoglobin level in the patients.

## Conclusion

Our findings suggest a spatially specific disruption of functional connectivity in the DMN in patients with ESRD, thereby providing novel insights into our understanding of the neuro-physiology mechanism that underlies the disease.

## Introduction

End-stage renal disease (ESRD) is a disease characterized by multi-organ dysfunction, which typically occurs when chronic renal failure progresses to a point where the kidneys are permanently functioning at less than 10% of their capacity [1]. ESRD is not only accompanied with central nervous system abnormalities (e.g., white matter lesions, cerebral atrophy and myelinoclasia) [2], but also results in various neurological problems (e.g., Wernicke's encephalopathy, uremic encephalopathy and dialysis encephalopathy) [3]. Moreover, ESRD significantly elevates the risk for developing cognitive impairments [4–6].

Recently, neuroimaging techniques have been used to investigate the neural mechanisms underlying ESRD-related neurological complications. For example, conventional MR imaging studies have shown that focal white matter lesions are more common in ESRD patients (56%) than in the normal population (27%) [7,8]. Based on single-photon emission computed tomography, arterial spin-labeling MR perfusion imaging and magnetic resonance spectroscopy, ESRD-related changes in cerebral metabolism and function have also been documented [9–11]. Further evidence from diffusion tensor imaging studies indicates that ESRD is associated with widespread disruptions of white matter integrity [12–14]. These studies collectively indicate the disorganized brain architecture induced by ESRD.

More recently, several groups have begun to apply resting-state functional magnetic resonance imaging (R-fMRI), a promising technique to depict intrinsic functional connectivity networks [15–17] to studies of ESRD [18–21]. With this technique, a consistent finding is disrupted functional integration of the default mode network (DMN) in ESRD [18,19,21,22], based on methods of regional homogeneity, independent component analysis or nodal centrality. It is well documented that the DMN is functionally heterogeneous with different connectivity profiles between its anterior and posterior parts [23–25]. However, whether and how the anterior and posterior components of the DMN are differentially involved in ESRD are largely unknown.

In the current study, we performed a whole-brain seed-based functional connectivity analysis of R-fMRI data collected from 31 neurologically asymptomatic patients with ESRD to investigate their functional connectivity maps of the DMN regions over the whole brain. Specifically, the seeds were centered at the posterior cingulate cortex (PCC) and ventromedial prefrontal cortex (vmPFC), respectively, to examine spatial specificity of ESRD-related alterations. Finally, ESRD-related functional connectivity alterations were correlated with neuropsychological tests and biomechanical variables of the patients.

## Materials and Methods

### Participants

This study was approved by the Research Ethics Review Board of Guangdong Provincial No.2 People's Hospital, and written informed consent was obtained from each participant. A total of thirty-four patients with ESRD (all right-handed) were enrolled in this study from the renal transplantation department of our hospital between August 2011 and July 2013. Exclusion

criteria included: (1) psychiatric disorders or major neurologic disorders (e.g., severe head injury, stroke, epilepsy, dementia, anxiety, depression or visible lesions) according to an experienced physician (G. X., with 20-year experience in neurology); (2) ischemic diseases including acute ischemic cerebrovascular disease, acute peripheral arterial occlusion, advanced liver or heart failure; (3) asymptomatic coronary ischemia by electrocardiogram testing; (4) a history of diabetes; and (5) substance abuse including drugs, alcohol or cigarettes. Conventional MR images were examined by an experienced radiologist (W. L., with 20 years of experience in neuropathology), who was blinded to whether the images were from the patient or control group. Three patients were excluded due to abnormal hyper-intensities in the T2-FLAIR MR images [3]. Therefore, the final study population included 31 patients with ESRD (24 men and 7 female, mean age  $39.9 \pm 9.6$  years, range 24–61 years).

Thirty-one age- and gender-matched HCs (all right-handed; 32 males; mean age  $41.5 \pm 10.6$  years, range 22–58 years) were recruited from the local community. All the HCs had no physical diseases or history of psychiatric or neurologic diseases.

All the participants underwent a neuropsychological test involving the mini-mental state examination (MMSE) [26], and the evaluation of systolic and diastolic blood pressure. ESRD group completed multiple biochemical tests after the hemodialysis (within 36 hours) but before the MR imaging (within 24 hours). The biochemical tests included Scr (serum creatinine), BUN (blood urea nitrogenurea), cholesterol, hemoglobin, serum kalium and serum calcium. Out of the 31 patients with ESRD, 20 (64.5%) had hypertension, and 6 (19.3%) had hyperlipidemia. In the current study, the patients with anemia were treated with ferrous succinate or polysaccharide iron complex.

All the demographic and clinical data are summarized in Table 1.

### Image acquisition

All participants were scanned on a 1.5-T MR scanner (Achieva Nova-Dual, Philips, Best, the Netherlands) in the Department of Medical Imaging center at Guangdong No. 2 Provincial

**Table 1. Demographics and clinical characteristics of all participants.**

	ESRD (n = 31)	HCs (n = 31)	P-value
Gender (M/F)	24/7	21/10	0.393 <sup>a</sup>
Age (years)	$39.9 \pm 9.6$ (24–61)	$42.7 \pm 8.5$ (26–61)	0.216 <sup>b</sup>
Education (years)	$11.8 \pm 3.3$ (3–16)	$10.8 \pm 2.8$ (6–16)	0.174 <sup>b</sup>
MMSE	$29.1 \pm 0.8$ (28–30)	$29.8 \pm 0.5$ (28–30)	<0.001 <sup>b</sup>
Systolic blood pressure	$172.9 \pm 9.6$ (160–180)	$100.9 \pm 7.2$ (90–115)	<0.001 <sup>b</sup>
Diastolic blood pressure	$95.4 \pm 6.1$ (85–100)	$70.7 \pm 5.9$ (60–80)	<0.001 <sup>b</sup>
Dialysis duration (months)	$16.0 \pm 6.6$ (6–30)		
Serum calcium (mmol/L)	$2.3 \pm 0.2$ (1.9–2.9)		
Serum kalium (mmol/L) <sup>c</sup>	$4.6 \pm 0.8$ (3.0–6.3)		
Hemoglobin (g/L) <sup>d</sup>	$104.0 \pm 24.7$ (56–158)		
Serum creatinine (μmol/L)	$783.3 \pm 402.2$ (86–1458)		
Blood urea nitrogenurea (mmol/L)	$17.7 \pm 8.1$ (4.1–30.3)		

Values are represented as mean ± SD (min—max). ESRD, end-stage renal disease; HCs, healthy controls; M, male; F, female; MMSE, the Mini-Mental Status Examination.

<sup>a</sup>The P-value was obtained by chi-square test.

<sup>b</sup>The P-values were obtained by two-side two-sample t tests.

<sup>c</sup>Data were missed for two patients.

<sup>d</sup>Data were missed for three patients.

doi:10.1371/journal.pone.0161392.t001

People's Hospital. None of the subjects were taking any medications at the time of the scans. The conventional imaging sequences, including T1-weighted images and T2-FLAIR images, were obtained for each participant to detect clinically silent lesions. During the R-fMRI data scanning, the participants were asked to lie quietly with their eyes closed and to not think of anything specific while in the scanner. The scan lasted 8 minutes, and 160 volumes were obtained for each participant. The R-fMRI acquisition parameters were as follows: 33 axial slices; repetition time (TR) = 3,000 ms; echo time (TE) = 50 ms; flip angle = 90°; slice thickness = 4.5 mm; no gap; matrix = 128 × 128 and field of view (FOV) = 230 × 230 mm<sup>2</sup>. After scanning, all the participants were asked questions to verify the degree of their cooperation. Additionally, individual high-resolution anatomical images were also acquired using a T1-weighted three-dimensional volumetric magnetization-prepared rapidly acquired gradient-echo sequence: 160 axial slices; TR = 25 ms; TE = 4.1 ms; FA = 30°; slice thickness = 1.0 mm; no gap; matrix = 256 × 256; and FOV = 230 × 230 mm<sup>2</sup>.

### Image preprocessing

Data preprocessing was performed using the SPM12 package (<http://www.fil.ion.ucl.ac.uk/spm/software/spm12/>) and GRETNA package [27], including i) removal of the first five volumes to allow T1 equilibration effects; ii) realignment to correct for spatial displacements due to head motion; iii) co-registration to structural images; iv) spatial normalization into the Montreal Neurological Institute space by applying deformation field derived from tissue segmentation of structural images; v) spatial smoothing (Gaussian kernel of 6-mm full width at half maximum); vi) removal of linear trend; vii) temporal band-pass filtering (0.01–0.1 Hz); and viii) regression of several nuisance signals of white matter signal, cerebrospinal fluid signal and head-motion profiles.

Recent studies have highlighted residual head-motion effects on intrinsic functional connectivity [15,28]. In the current study, we first excluded participants with head motion > 3 mm of displacement or > 3 degree of rotation in any direction. Then, we examined both gross (i.e., maximum and root mean square) and micro (mean frame-wise displacement) head-motion summary measures and found no significant between-group differences (all *P*s > 0.05). Furthermore, we employed a 24-parameter instead of 6-parameter head-motion model during the regression of nuisance signals [29], an efficiency strategy to control for head motion effects [30]. Finally, we treated all the summary head-motion measures as covariates at the group-level comparisons [31]. After these efforts, we believe that head-motion effects were mitigated as much as possible for the current data. Of note, how to attenuate head-motion effects is an ongoing topic of research, and there are other alternative strategies to deal with this issue [32,33].

### Seed-based functional connectivity

Although typically regarded as a homogenous network, the DMN is functionally heterogeneous, with particularly striking differences in connectivity patterns between the anterior and posterior DMN [23]. Thus, in the current study, we studied functional connectivity of both anterior and posterior DMN by locating the seeds in the PCC (Talairach coordinates = [-2-51 27]) and vmPFC (Talairach coordinates [2 54-3]), respectively [23]. Their counterparts in the MNI space converted according to [34] were then used as centers to generate two spherical regions of interest (ROIs) with radius = 6 mm. For each participant, a reference time series was then obtained for each ROI by averaging all the voxels' time series within it. The resulting reference time series were further correlated with the time series over the entire brain in a voxel-wise manner, thereby generating two functional connectivity maps individually. Finally, a Fisher's *r*-to-*z* transformation was applied to the resulting whole-brain correlation maps to improve the normality of the correlation coefficients.

## Statistical analysis

**Functional connectivity map and between-group difference.** For each group, a random-effect one-sample t-test was performed in a voxel-wise manner to determine regions that showed functional connectivity with the seeds (i.e., PCC and vmPFC). A random field theory as performed in the SPM toolbox was used to account for the multiple comparison issue ( $P < 0.05$ , corrected, cluster size  $> 10$  voxels). To further identify regions whose functional connectivity with the seeds differed between the ESRD and HC groups, a voxel-wise multiple general linear model was implemented with age, gender, education and summary head-motion measures as covariates. To correct for the multiple comparison issue, the Alpha-Sim procedure [35] was implemented in the REST by combining the height threshold of  $P < 0.001$  [36] and extent threshold of  $P < 0.05$ , which corresponded to a corrected  $P < 0.05$ . All the results were mapped onto the cortical surfaces for visualization using the BrainNet Viewer package [37].

**Brain-behavior relationship.** For each region showing significantly different functional connectivity between the ESRD and HC controls, the Pearson correlation coefficient was calculated to assess the relationship between mean function connectivity strength of the region (after Fisher's  $r$ -to- $z$  transformation) and clinical variables (dialysis duration, calcium level, kalium level, hemoglobin level, creatinine level and urea level) in the patient group.

## Results

### Demographic and clinical characteristics

The demographic, biochemical and clinical characteristics for all the participants are shown in [Table 1](#). There were no significant differences in gender ( $P = 0.393$ ), age ( $P = 0.216$ ) or education level ( $P = 0.174$ ) between the ESRD and HC groups. Compared with the HCs, the ESRD patients had significantly higher systolic and diastolic blood pressure values and lower MMSE scores ( $P < 0.001$ ). The mean duration of hemodialysis for the patient group was  $16.0 \pm 6.6$  months. The mean calcium, kalium, hemoglobin, creatinine, and urea levels for the patients were  $2.3 \pm 0.2$  mmol/L,  $4.6 \pm 0.8$  mmol/L,  $104.0 \pm 24.7$ g/L,  $783.3 \pm 402.2$   $\mu$ mol/L and  $17.7 \pm 8.1$  mmol/L, respectively. Notably, the serum calcium levels were corrected with serum albumin levels using the Payne's formula [38].

### Functional connectivity maps

[Fig 1](#) shows the DMN functional connectivity patterns for the ESRD and HC groups and between-group differences. Overall, our PCC-based and vmPFC-based functional connectivity analyses largely replicated numerous previous studies of the DMN topography that predominantly embraced the medial prefrontal cortex, dorsolateral prefrontal cortex, lateral temporal cortex, and post-medial parietal cortex. We also note that PCC-based functional connectivity analysis revealed a spatially more extensive DMN pattern relative to the vmPFC.

Compared with the HC, four clusters were found to show significantly decreased functional connectivity with the PCC in the patients with ESRD, involving the left middle temporal gyrus, the right anterior cingulate gyrus, and the bilateral medial superior frontal gyri. For the vmPFC seed, only the right thalamus showed significantly decreased functional connectivity in patients with ESRD compared to HCs ([Fig 1](#)).

### Relationship between DMN functional connectivity and clinical variables

Functional connectivity between the PCC and right medial superior frontal gyrus exhibited a significantly positive correlation with the hemoglobin level ( $r = 0.489$ ,  $P = 0.008$ ) ([Fig 2](#)). We

did not correlate ESRD-related functional connectivity alterations with the MMSE scores in the patients due to the narrow range distribution of the values (28–30).

### Reproducibility analyses

In the current study, we noted that two patients had very low hemoglobin values (56 g/L and 59 g/L), suggesting severe anemia. Therefore, we reanalyzed our data after excluding these two patients to test the extent to which our main findings were affected. We found that the results were largely preserved for both whole-brain functional connectivity differences (Fig 3) and MRI-clinical correlations ( $r = 0.590, P = 0.002$ ). In addition, for the ESRD patients included in the current study, 20 (64.5%) had hypertension and 6 (19.3%) had hyperlipidemia. Thus, we further compared the functional connectivity between the ESRD patients with hypertension/hyperlipidemia and those without hypertension/hyperlipidemia for each cluster that exhibited functional connectivity differences between the ESRD and HC groups. No significant differences were found for any cluster ( $P > 0.05$ ). Furthermore, we performed a voxel-wise comparison of whole-brain functional connectivity between the ESRD patients with hypertension/hyperlipidemia and those without hypertension/hyperlipidemia. Again, no significant differences were observed ( $P > 0.05$ , corrected with the Alpha-Sim procedure). All these reproducibility analyses indicate little effects of anemia, hypertension and hyperlipidemia on the reported results.

### Discussion

This study employed R-fMRI to evaluate the DMN functional connectivity in patients with ESRD. Although typically regarded as a homogenous network, accumulating evidence

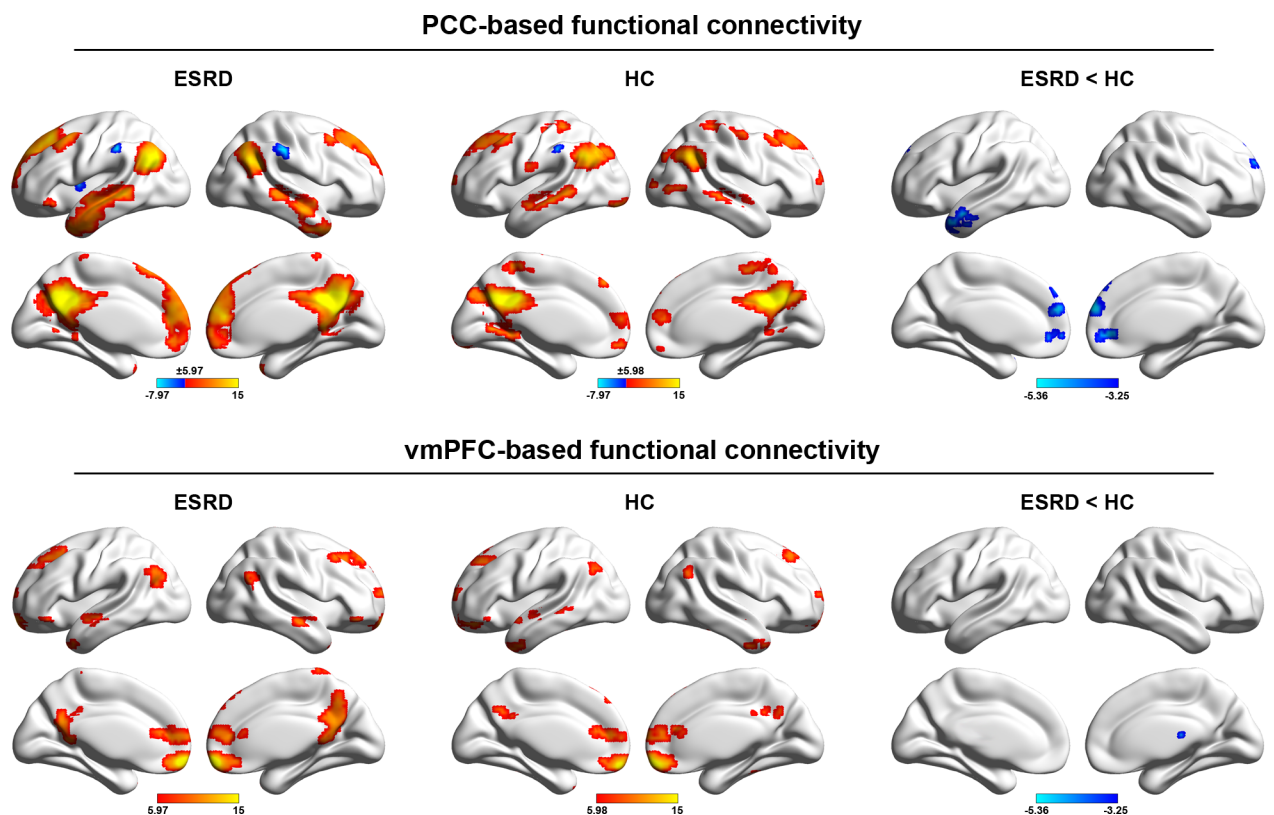


**Fig 1. Within-group DMN patterns and between-group differences.** The color bars represent the T scores. The results were mapped onto the brain surface using the BrainNet viewer software.

doi:10.1371/journal.pone.0161392.g001

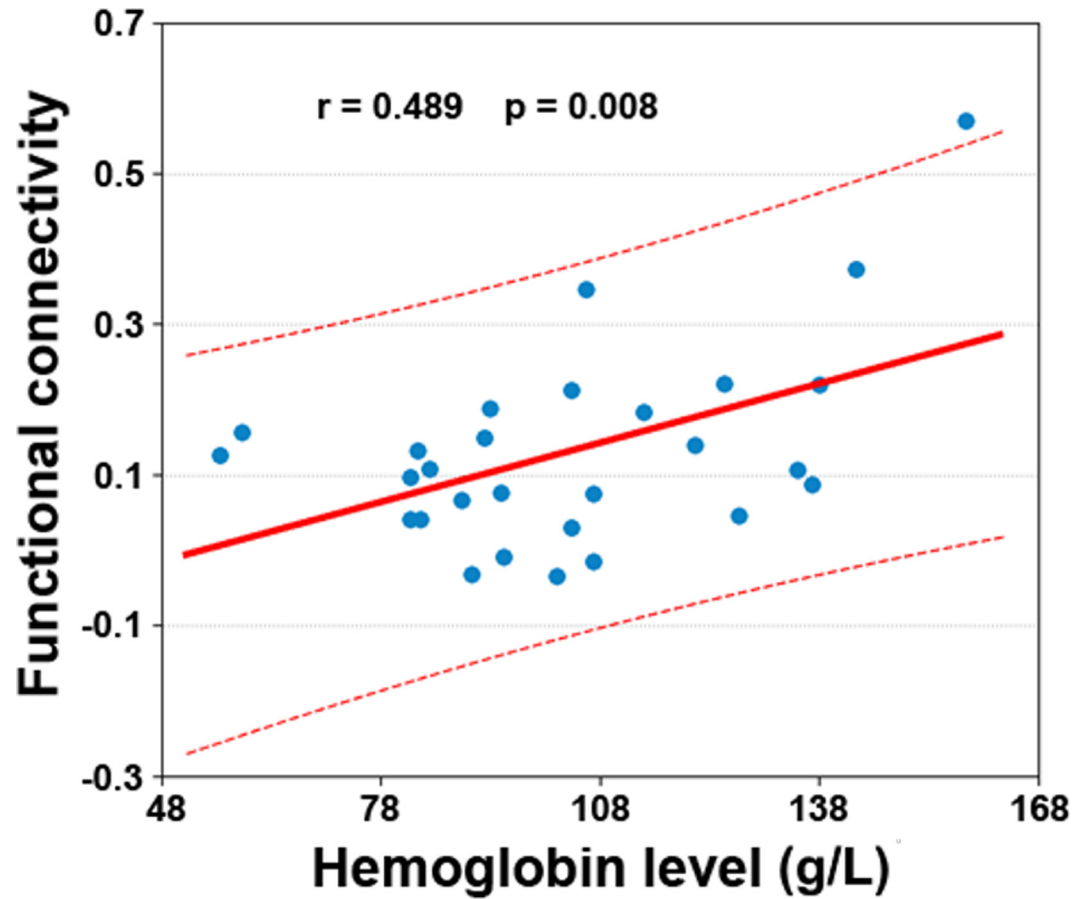


**Fig 2. Scatter plot of the relationship between the PCC-right medial superior frontal gyrus functional connectivity and hemoglobin levels in the patients.**

doi:10.1371/journal.pone.0161392.g002

indicates functional heterogeneity within the DMN. Specifically, evidence from task-based activation studies shows that the anterior vmPFC and posterior PCC, two key nodes within the DMN, act independently across a wide array of cognitive tasks. Moreover, functional

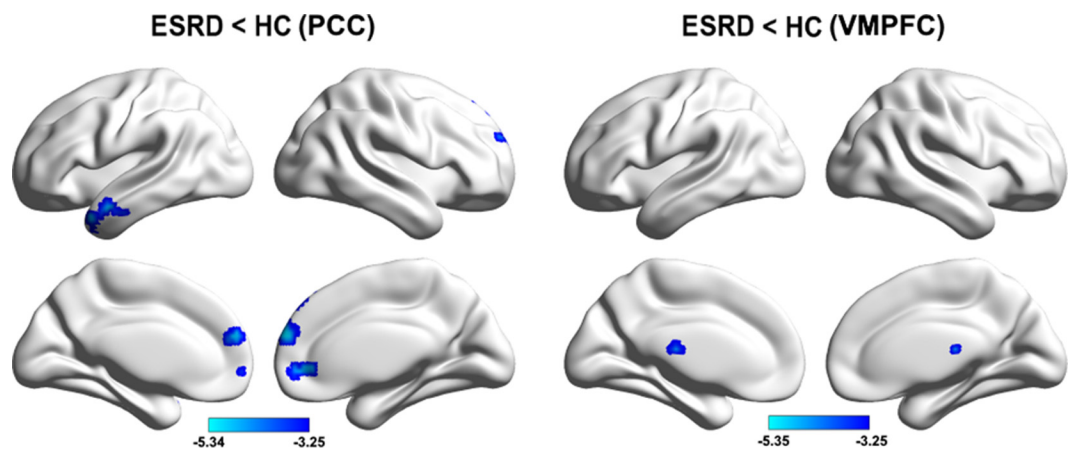


**Fig 3. Between-group functional connectivity differences after excluding two patients with anemia.**

doi:10.1371/journal.pone.0161392.g003

connectivity studies from both resting state and cognitive tasks reveal different connectivity patterns between the vmPFC and PCC [23–25]. The anterior-posterior functional dissociation within the DMN implies differences in their interactions with other networks and highlights the need for researchers to treat them individually. In response, we examined both anterior and posterior DMN functional connectivity in ESRD by seeding the ROIs in the PCC and vmPFC, respectively. We found that patients with ESRD mainly exhibited decreased within-DMN functional connectivity when the seed was located in the PCC while decreased frontal-subcortical functional connectivity was determined when the seed was located in the vmPFC. These findings provide new insights into our understanding of neural abnormalities in ESRD.

We found that compared with HCs, patients with ESRD showed decreased functional connectivity in the anterior cingulate cortex, middle temporal gyrus and medial superior frontal cortex when the seed was located in the PCC. These structures are typical DMN components, suggesting decreased within-DMN functional integration in ESRD. This is consistent with previous R-fMRI studies based on regional homogeneity [18] and independent component analysis methods [19] in ESRD. Using MR spectroscopy [11,39], diffusion-tensor imaging [14], and voxel-based morphometry [10], many previous studies have demonstrated ESRD-related abnormalities in brain biochemistry and structure of multiple DMN regions. These abnormalities may be the possible biochemical and/or structural basis for the disrupted DMN functional connectivity observed here. Functionally, the DMN is engaged in a broad array of cognitive processing related to self-awareness, episodic memory, and interactive modulation between the internal brain activities and external tasks [40,41]. Before any overt neurological manifestation, patients with ESRD often develop various cognitive deficits involving attention, processing speed [42], executive function [4], and memory [43]. Thus, we speculated that the decreased within-DMN functional integration might in part underlie these cognitive disturbances in ESRD. Future follow-up studies are required to provide more complete neuropsychological test of ESRD to find the real relation between the neuropsychological test in ESRD patients and DMN.

Interestingly, we found a positive correlation between PCC-medial superior frontal gyrus function connectivity and the hemoglobin levels in patients with ESRD. Previous studies have shown that long-term hemodialysis could lead to cerebral abnormalities of oxygenation [10] and cerebral blood flow in ESRD [44–46], which could significantly affect the brain function and cerebral circulation [47–50]. Recent studies have highlighted important roles of cerebral blood flow and metabolism in establishing and retaining interregional functional coordination in the brain [51,52]. Given previous findings that low hemoglobin is associated with poor mental health in ESRD [46,53,54], further insights into this issue could benefit from simultaneously recording MR spectroscopy, ASL perfusion, R-fMRI, and neuropsychological data of the same cohort of patients in future.

When seeded in the vmPFC, patients with ESRD were found to show decreased functional connectivity with the thalamus. vmPFC is a key structure implicated in emotional and cognitive processing by interacting with a number of subcortical structures, including the thalamus [23,55,56]. Therefore, disruption of both structural and functional connectivity between the thalamus and frontal DMN regions are frequently reported for depressive individuals [57,58]. Patients with ESRD typically present with mood-related problems, such as adaptive behavior of fear. Previous studies have shown that the paraventricular nucleus of the thalamus (PVT), one putative stress sensor [59,60], constitutes a novel circuit essential for establishment of fear memory, the expression of fear responses and adaptive behavior of fear [61]. Moreover, ESRD patients are prone to develop depression [62]. Thus, we deduce that the decreased functional connectivity between the vmPFC and the thalamus observed here may account for neurocognitive dysfunctions and in particular mood-related processing (e.g., adaptive behavior of fear),

which ultimately contribute to the susceptibility of ESRD patients to develop depression. If this deduction holds true, an interesting future topic is to test whether cognitive training that can enhance the thalamic and DMN functional connectivity may improve cognitive function in patients with ESRD. However, there is another possibility that the current patients may be complicated by depression, which further leads to the observed functional connectivity decrease between the vmPFC and thalamus. Future studies are needed to clarify this issue.

## Limitations

First, the sample size was relatively small and the MRI scanning parameters were suboptimal (e.g., 1.5T scanner and anisotropic voxels) for the current dataset. However, our previous studies based on this dataset consistently demonstrate ESRD-related functional connectivity disruptions of the DMN [21,22], which are largely comparable with studies utilizing optimal imaging parameters on 3T MRI scanners [18,19]. This implies the validity of the current dataset to study functional connectivity of the DMN in ESRD. Nevertheless, we want to emphasize that future studies with a large cohort of participants are needed to examine the reproducibility of our findings using more advanced techniques and optimized parameters. Second, due to the cross-sectional design of the current study, we cannot address how the DMN functional connectivity changes dynamically in response to the progression of chronic kidney disease (CKD). Thus, future longitudinal studies addressing DMN functional connectivity and changes in neuropsychological tests in CKD patients with different degrees of kidney function may provide further insight on the time course of alterations in brain functional connectivity and neuropsychological behavior as kidney function deteriorates. Third, consistent with a recent fMRI study [19], several comorbidities associated with ESRD (e.g., anemia, hypertension and hyperlipidemia) existed for the patients in the current study. Therefore, it is likely that the observed DMN function connectivity abnormalities are a common consequence of both ESRD and these comorbidities. Although our exploratory analyses revealed non-significant effects of these factors on our results, it may be due to the small sample size. Given the influences of these factors on BOLD signals [63,64], it is an interesting topic in the future to systematically investigate how these factors impact functional networks of the brain. Additionally, it should be noted that there are still other factors that may contribute to the current findings given the end stage of the disease, such as depression, a common complication in ESRD. However, the current samples did not undergo neuropsychological tests for these psychological disorders, thus our findings should be interpreted with caution. Finally, we did not collect clinical information such as hematocrit, mean hemodialysis session duration and prevalence of intradialytic hypotension for the patients, limiting us to examine how ESRD-related functional connectivity alterations are related to these specific clinical variables in the patients. Future studies can address these important issues by using more rigorous experimental design and stricter enrollment criteria. Finally, accumulating evidence suggests that the DMN functional connectivity reflects underlying structural pathways [59, 60]. Therefore, it would be interesting to study whether the disrupted DMN functional connectivity observed here has a structural substrate.

## Conclusion

The current study demonstrates the disconnectivity between the PCC and the anterior cingulate and middle temporal gyrus regions, the vmPFC and the thalamus in the brain of patients with ESRD. Moreover, the disconnectivity is related to biochemical parameters in these patients. These findings provide novel insights into the neurophysiological mechanism of asymptomatic patients with ESRD.

## Acknowledgments

We thank all the patients and volunteers for participating in this study. This work was supported by grants from National Natural Science Foundation of China (No. 81471639); The Science and Technology Planning Project of Guangdong Province, China (No. 2015A030313723).

## Author Contributions

**Formal analysis:** XM JD.

**Funding acquisition:** GJ.

**Investigation:** YX.

**Methodology:** XM GJ JD WZ JT XZ.

**Project administration:** XM JT ZW.

**Software:** XM GJ JD WZ JT XZ.

**Supervision:** GJ ZL.

**Writing – original draft:** XM.

## References

1. Foley RN, Collins AJ (2007) End-stage renal disease in the United States: an update from the United States Renal Data System. *J Am Soc Nephrol* 18: 2644–2648. PMID: [17656472](#)
2. De Deyn PP, Saxena VK, Abts H, Borggreve F, D'Hooge R, Marescau B, et al. (1992) Clinical and pathophysiological aspects of neurological complications in renal failure. *Acta Neurol Belg* 92: 191–206. PMID: [1332359](#)
3. Brouns R, De Deyn PP (2004) Neurological complications in renal failure: a review. *Clin Neurol Neurosurg* 107: 1–16. PMID: [15567546](#)
4. Kurella M, Chertow GM, Luan J, Yaffe K (2004) Cognitive impairment in chronic kidney disease. *J Am Geriatr Soc* 52: 1863–1869. PMID: [15507063](#)
5. Murray AM, Tupper DE, Knopman DS, Gilbertson DT, Pederson SL, Li S, et al. (2006) Cognitive impairment in hemodialysis patients is common. *Neurology* 67: 216–223. PMID: [16864811](#)
6. Kurella Tamura M, Yaffe K (2011) Dementia and cognitive impairment in ESRD: diagnostic and therapeutic strategies. *Kidney Int* 79: 14–22. doi: [10.1038/ki.2010.336](#) PMID: [20861818](#)
7. Agildere AM, Kurt A, Yildirim T, Benli S, Altinors N (2001) MRI of neurologic complications in end-stage renal failure patients on hemodialysis: pictorial review. *Eur Radiol* 11: 1063–1069. PMID: [11419154](#)
8. Martinez-Vea A, Salvado E, Bardaji A, Gutierrez C, Ramos A, Garcia C, et al. (2006) Silent cerebral white matter lesions and their relationship with vascular risk factors in middle-aged predialysis patients with CKD. *Am J Kidney Dis* 47: 241–250. PMID: [16431253](#)
9. Fazekas G, Fazekas F, Schmidt R, Kapeller P, Offenbacher H, Krejs G (1995) Brain MRI findings and cognitive impairment in patients undergoing chronic hemodialysis treatment. *J Neurol Sci* 134: 83–88. PMID: [8747848](#)
10. Prohovnik I, Post J, Uribarri J, Lee H, Sandu O, Langhoff E (2007) Cerebrovascular effects of hemodialysis in chronic kidney disease. *J Cereb Blood Flow Metab* 27: 1861–1869. PMID: [17406658](#)
11. Tryc AB, Alwan G, Bokemeyer M, Goldbecker A, Hecker H, Haubitz M (2011) Cerebral metabolic alterations and cognitive dysfunction in chronic kidney disease. *Nephrol Dial Transplant* 26: 2635–2641. doi: [10.1093/ndt/gfq729](#) PMID: [21216887](#)
12. Hsieh TJ, Chang JM, Chuang HY, Ko CH, Hsieh ML, Liu GC, et al. (2009) End-stage renal disease: in vivo diffusion-tensor imaging of silent white matter damage. *Radiology* 252: 518–525. doi: [10.1148/radiol.2523080484](#) PMID: [19528357](#)
13. Chou MC, Hsieh TJ, Lin YL, Hsieh YT, Li WZ, Chang JM, et al. (2013) Widespread white matter alterations in patients with end-stage renal disease: a voxelwise diffusion tensor imaging study. *AJNR Am J Neuroradiol* 34: 1945–1951. doi: [10.3174/ajnr.A3511](#) PMID: [23788598](#)

14. Kim HS, Park JW, Bai DS, Jeong JY, Hong JH, Son SM, et al. (2011) Diffusion tensor imaging findings in neurologically asymptomatic patients with end stage renal disease. *NeuroRehabilitation* 29: 111–116. doi: [10.3233/NRE-2011-0684](https://doi.org/10.3233/NRE-2011-0684) PMID: [21876303](https://pubmed.ncbi.nlm.nih.gov/21876303/)
15. Van Dijk KR, Hedden T, Venkataraman A, Evans KC, Lazar SW, Buckner RL (2010) Intrinsic functional connectivity as a tool for human connectomics: theory, properties, and optimization. *J Neurophysiol* 103: 297–321. doi: [10.1152/jn.00783.2009](https://doi.org/10.1152/jn.00783.2009) PMID: [19889849](https://pubmed.ncbi.nlm.nih.gov/19889849/)
16. Wang J, Zuo X, He Y (2010) Graph-based network analysis of resting-state functional MRI. *Front Syst Neurosci* 4: 16. doi: [10.3389/fnsys.2010.00016](https://doi.org/10.3389/fnsys.2010.00016) PMID: [20589099](https://pubmed.ncbi.nlm.nih.gov/20589099/)
17. Biswal B, Yetkin FZ, Haughton VM, Hyde JS (1995) Functional connectivity in the motor cortex of resting human brain using echo-planar MRI. *Magn Reson Med* 34: 537–541. PMID: [8524021](https://pubmed.ncbi.nlm.nih.gov/8524021/)
18. Liang X, Wen J, Ni L, Zhong J, Qi R, Zhang LJ, et al. (2013) Altered pattern of spontaneous brain activity in the patients with end-stage renal disease: a resting-state functional MRI study with regional homogeneity analysis. *PLoS One* 8: e71507. doi: [10.1371/journal.pone.0071507](https://doi.org/10.1371/journal.pone.0071507) PMID: [23990958](https://pubmed.ncbi.nlm.nih.gov/23990958/)
19. Ni L, Wen J, Zhang LJ, Zhu T, Qi R, Xu Q, et al. (2014) Aberrant default-mode functional connectivity in patients with end-stage renal disease: a resting-state functional MR imaging study. *Radiology* 271: 543–552. doi: [10.1148/radiol.13130816](https://doi.org/10.1148/radiol.13130816) PMID: [24484062](https://pubmed.ncbi.nlm.nih.gov/24484062/)
20. Qiu Y, Lv X, Su H, Jiang G, Li C, Tian J (2014) Structural and functional brain alterations in end stage renal disease patients on routine hemodialysis: a voxel-based morphometry and resting state functional connectivity study. *PLoS One* 9: e98346. doi: [10.1371/journal.pone.0098346](https://doi.org/10.1371/journal.pone.0098346) PMID: [24854737](https://pubmed.ncbi.nlm.nih.gov/24854737/)
21. Ma X, Jiang G, Li S, Wang J, Zhan W, Zeng S, et al. (2015) Aberrant functional connectome in neurologically asymptomatic patients with end-stage renal disease. *PLoS One* 10: e0121085. doi: [10.1371/journal.pone.0121085](https://doi.org/10.1371/journal.pone.0121085) PMID: [25786231](https://pubmed.ncbi.nlm.nih.gov/25786231/)
22. Li S, Ma X, Huang R, Li M, Tian J, Wen H, et al. (2016) Abnormal degree centrality in neurologically asymptomatic patients with end-stage renal disease: A resting-state fMRI study. *Clin Neurophysiol* 127: 602–609. doi: [10.1016/j.clinph.2015.06.022](https://doi.org/10.1016/j.clinph.2015.06.022) PMID: [26160274](https://pubmed.ncbi.nlm.nih.gov/26160274/)
23. Uddin LQ, Kelly AM, Biswal BB, Castellanos FX, Milham MP (2009) Functional connectivity of default mode network components: correlation, anticorrelation, and causality. *Hum Brain Mapp* 30: 625–637. doi: [10.1002/hbm.20531](https://doi.org/10.1002/hbm.20531) PMID: [18219617](https://pubmed.ncbi.nlm.nih.gov/18219617/)
24. Mitchell JP, Heatherton TF, Macrae CN (2002) Distinct neural systems subserve person and object knowledge. *Proc Natl Acad Sci U S A* 99: 15238–15243. PMID: [12417766](https://pubmed.ncbi.nlm.nih.gov/12417766/)
25. Cavanna AE, Trimble MR (2006) The precuneus: a review of its functional anatomy and behavioural correlates. *Brain* 129: 564–583. PMID: [16399806](https://pubmed.ncbi.nlm.nih.gov/16399806/)
26. Schultz-Larsen K, Lomholt RK, Kreiner S (2007) Mini-Mental Status Examination: a short form of MMSE was as accurate as the original MMSE in predicting dementia. *J Clin Epidemiol* 60: 260–267. PMID: [17292020](https://pubmed.ncbi.nlm.nih.gov/17292020/)
27. Wang J, Wang X, Xia M, Liao X, Evans A, He Y (2015) GRETNA: a graph theoretical network analysis toolbox for imaging connectomics. *Front Hum Neurosci* 9: 386. doi: [10.3389/fnhum.2015.00386](https://doi.org/10.3389/fnhum.2015.00386) PMID: [26175682](https://pubmed.ncbi.nlm.nih.gov/26175682/)
28. Power JD, Barnes KA, Snyder AZ, Schlaggar BL, Petersen SE (2012) Spurious but systematic correlations in functional connectivity MRI networks arise from subject motion. *Neuroimage* 59: 2142–2154. doi: [10.1016/j.neuroimage.2011.10.018](https://doi.org/10.1016/j.neuroimage.2011.10.018) PMID: [22019881](https://pubmed.ncbi.nlm.nih.gov/22019881/)
29. Friston KJ, Holmes A, Poline JB, Price CJ, Frith CD (1996) Detecting activations in PET and fMRI: levels of inference and power. *Neuroimage* 4: 223–235. PMID: [9345513](https://pubmed.ncbi.nlm.nih.gov/9345513/)
30. Yan CG, Craddock RC, He Y, Milham MP (2013) Addressing head motion dependencies for small-world topologies in functional connectomics. *Front Hum Neurosci* 7: 910. doi: [10.3389/fnhum.2013.00910](https://doi.org/10.3389/fnhum.2013.00910) PMID: [24421764](https://pubmed.ncbi.nlm.nih.gov/24421764/)
31. Fair DA, Nigg JT, Iyer S, Bathula D, Mills KL, Dosenbach NU, et al. (2012) Distinct neural signatures detected for ADHD subtypes after controlling for micro-movements in resting state functional connectivity MRI data. *Front Syst Neurosci* 6: 80. doi: [10.3389/fnsys.2012.00080](https://doi.org/10.3389/fnsys.2012.00080) PMID: [23382713](https://pubmed.ncbi.nlm.nih.gov/23382713/)
32. Muschelli J, Nebel MB, Caffo BS, Barber AD, Pekar JJ, Mostofsky SH (2014) Reduction of motion-related artifacts in resting state fMRI using aCompCor. *Neuroimage* 96: 22–35. doi: [10.1016/j.neuroimage.2014.03.028](https://doi.org/10.1016/j.neuroimage.2014.03.028) PMID: [24657780](https://pubmed.ncbi.nlm.nih.gov/24657780/)
33. Patel AX, Kundu P, Rubinov M, Jones PS, Vertes PE, Ersche KD, et al. (2014) A wavelet method for modeling and despiking motion artifacts from resting-state fMRI time series. *Neuroimage* 95: 287–304. doi: [10.1016/j.neuroimage.2014.03.012](https://doi.org/10.1016/j.neuroimage.2014.03.012) PMID: [24657353](https://pubmed.ncbi.nlm.nih.gov/24657353/)
34. Lancaster JL, Tordesillas-Gutierrez D, Martinez M, Salinas F, Evans A, Zilles K, et al. (2007) Bias between MNI and Talairach coordinates analyzed using the ICBM-152 brain template. *Hum Brain Mapp* 28: 1194–1205. PMID: [17266101](https://pubmed.ncbi.nlm.nih.gov/17266101/)

35. Ledberg A, Akerman S, Roland PE (1998) Estimation of the probabilities of 3D clusters in functional brain images. *Neuroimage* 8: 113–128. PMID: [9740755](#)
36. Woo CW, Krishnan A, Wager TD (2014) Cluster-extent based thresholding in fMRI analyses: pitfalls and recommendations. *Neuroimage* 91: 412–419. doi: [10.1016/j.neuroimage.2013.12.058](#) PMID: [24412399](#)
37. Xia M, Wang J, He Y (2013) BrainNet Viewer: a network visualization tool for human brain connectomics. *PLoS One* 8: e68910. doi: [10.1371/journal.pone.0068910](#) PMID: [23861951](#)
38. Payne RB, Little AJ, Williams RB, Milner JR (1973) Interpretation of serum calcium in patients with abnormal serum proteins. *Br Med J* 4: 643–646. PMID: [4758544](#)
39. Chiu ML, Li CW, Chang JM, Chiang IC, Ko CH, Chuang HY, et al. (2010) Cerebral metabolic changes in neurologically presymptomatic patients undergoing haemodialysis: in vivo proton MR spectroscopic findings. *Eur Radiol* 20: 1502–1507. doi: [10.1007/s00330-009-1673-2](#) PMID: [19997847](#)
40. Buckner RL, Andrews-Hanna JR, Schacter DL (2008) The brain's default network: anatomy, function, and relevance to disease. *Ann N Y Acad Sci* 1124: 1–38. doi: [10.1196/annals.1440.011](#) PMID: [18400922](#)
41. Fox MD, Snyder AZ, Vincent JL, Corbetta M, Van Essen DC, Raichle ME (2005) The human brain is intrinsically organized into dynamic, anticorrelated functional networks. *Proc Natl Acad Sci U S A* 102: 9673–9678. PMID: [15976020](#)
42. Jassal SV, Roscoe J, LeBlanc D, Devins GM, Rourke S (2008) Differential impairment of psychomotor efficiency and processing speed in patients with chronic kidney disease. *Int Urol Nephrol* 40: 849–854. doi: [10.1007/s11255-008-9375-2](#) PMID: [18443915](#)
43. Williams MA, Sklar AH, Burright RG, Donovan PJ (2004) Temporal effects of dialysis on cognitive functioning in patients with ESRD. *Am J Kidney Dis* 43: 705–711. PMID: [15042548](#)
44. Holzer H, Marguc K, Poggliusch H, Ott E, Katschnig H (1981) The effects of haemodialysis on cerebral blood flow. *Proc Eur Dial Transplant Assoc* 18: 126–132. PMID: [7329959](#)
45. Stefanidis I, Bach R, Mertens PR, Liakopoulos V, Liapi G, Mann H, et al. (2005) Influence of hemodialysis on the mean blood flow velocity in the middle cerebral artery. *Clin Nephrol* 64: 129–137. PMID: [16114789](#)
46. Regolisti G, Maggiore U, Cademartiri C, Cabassi A, Caiazza A, Morabito S, et al. (2013) Cerebral blood flow decreases during intermittent hemodialysis in patients with acute kidney injury, but not in patients with end-stage renal disease. *Nephrol Dial Transplant* 28: 79–85. doi: [10.1093/ndt/gfs182](#) PMID: [22711517](#)
47. Gottlieb D, Mildworf B, Rubinger D, Melamed E (1987) The regional cerebral blood flow in patients under chronic hemodialytic treatment. *J Cereb Blood Flow Metab* 7: 659–661. PMID: [3654805](#)
48. Lindegaard KF, Lundar T, Wiberg J, Sjoberg D, Aaslid R, Normes H (1987) Variations in middle cerebral artery blood flow investigated with noninvasive transcranial blood velocity measurements. *Stroke* 18: 1025–1030. PMID: [2961104](#)
49. Postiglione A, Faccenda F, Gallotta G, Rubba P, Federico S (1991) Changes in middle cerebral artery blood velocity in uremic patients after hemodialysis. *Stroke* 22: 1508–1511. PMID: [1962325](#)
50. Hata R, Matsumoto M, Handa N, Terakawa H, Sugitani Y, Kamada T (1994) Effects of hemodialysis on cerebral circulation evaluated by transcranial Doppler ultrasonography. *Stroke* 25: 408–412. PMID: [7905681](#)
51. Liang X, Zou Q, He Y, Yang Y (2013) Coupling of functional connectivity and regional cerebral blood flow reveals a physiological basis for network hubs of the human brain. *Proc Natl Acad Sci U S A* 110: 1929–1934. doi: [10.1073/pnas.1214900110](#) PMID: [23319644](#)
52. Tomasi D, Wang GJ, Volkow ND (2013) Energetic cost of brain functional connectivity. *Proc Natl Acad Sci U S A* 110: 13642–13647. doi: [10.1073/pnas.1303346110](#) PMID: [23898179](#)
53. Bornivelli C, Aperis G, Giannikouris I, Paliouras C, Alivanis P (2012) Relationship between depression, clinical and biochemical parameters in patients undergoing haemodialysis. *J Ren Care* 38: 93–97. doi: [10.1111/j.1755-6686.2012.00259.x](#) PMID: [22429274](#)
54. Kalender B, Ozdemir AC, Koroglu G (2006) Association of depression with markers of nutrition and inflammation in chronic kidney disease and end-stage renal disease. *Nephron Clin Pract* 102: c115–121. PMID: [16282695](#)
55. Myers-Schulz B, Koenigs M (2012) Functional anatomy of ventromedial prefrontal cortex: implications for mood and anxiety disorders. *Mol Psychiatry* 17: 132–141. doi: [10.1038/mp.2011.88](#) PMID: [21788943](#)
56. Motzkin JC, Philippi CL, Oler JA, Kalin NH, Baskaya MK, Koenigs M (2015) Ventromedial prefrontal cortex damage alters resting blood flow to the bed nucleus of stria terminalis. *Cortex* 64: 281–288. doi: [10.1016/j.cortex.2014.11.013](#) PMID: [25569763](#)

57. Greicius MD, Flores BH, Menon V, Glover GH, Solvason HB, Kenna H, et al. (2007) Resting-state functional connectivity in major depression: abnormally increased contributions from subgenual cingulate cortex and thalamus. *Biol Psychiatry* 62: 429–437. PMID: [17210143](#)
58. Korgaonkar MS, Fornito A, Williams LM, Grieve SM (2014) Abnormal structural networks characterize major depressive disorder: a connectome analysis. *Biol Psychiatry* 76: 567–574. doi: [10.1016/j.biopsych.2014.02.018](#) PMID: [24690111](#)
59. Spencer SJ, Fox JC, Day TA (2004) Thalamic paraventricular nucleus lesions facilitate central amygdala neuronal responses to acute psychological stress. *Brain Res* 997: 234–237. PMID: [14706875](#)
60. Chastrette N, Pfaff DW, Gibbs RB (1991) Effects of daytime and nighttime stress on Fos-like immunoreactivity in the paraventricular nucleus of the hypothalamus, the habenula, and the posterior paraventricular nucleus of the thalamus. *Brain Res* 563: 339–344. PMID: [1786549](#)
61. Penzo MA, Robert V, Tucciarone J, De Bundel D, Wang M, Van Aelst L, et al. (2015) The paraventricular thalamus controls a central amygdala fear circuit. *Nature*.
62. Kimmel PL, Cukor D, Cohen SD, Peterson RA (2007) Depression in end-stage renal disease patients: a critical review. *Adv Chronic Kidney Dis* 14: 328–334. PMID: [17904499](#)
63. Son SJ, Kim J, Lee E, Park JY, Namkoong K, Hong CH, et al. (2015) Effect of hypertension on the resting-state functional connectivity in patients with Alzheimer's disease (AD). *Arch Gerontol Geriatr* 60: 210–216. doi: [10.1016/j.archger.2014.09.012](#) PMID: [25307953](#)
64. Li X, Liang Y, Chen Y, Zhang J, Wei D, Chen K, et al. (2015) Disrupted Frontoparietal Network Mediates White Matter Structure Dysfunction Associated with Cognitive Decline in Hypertension Patients. *J Neurosci* 35: 10015–10024. doi: [10.1523/JNEUROSCI.5113-14.2015](#) PMID: [26157001](#)